ACS APPLIED MATERIALS & INTERFACES

Research Article

www.acsami.org

# Spatial Atmospheric Atomic Layer Deposition of $In_xGa_yZn_zO$ for Thin Film Transistors

A. Illiberi,*[,†] B. Cobb,[†] A. Sharma,[†] T. Grehl,[‡] H. Brongersma,[‡,§] F. Roozeboom,[†,§] G. Gelinck,[†] and P. Poodt[†]

[†]Holst Centre/TNO, High Tech Campus 31, 5600 AE Eindhoven, The Netherlands

[‡]ION-TOF GmbH, Heisenbergstrasse 15, 48149, Muenster, Germany

[§]Department of Applied Physics, Eindhoven University of Technology, 5600 MB Eindhoven, The Netherlands

**ABSTRACT:** We have investigated the nucleation and growth of InGaZnO thin films by spatial atmospheric atomic layer deposition. Diethyl zinc (DEZ), trimethyl indium (TMIn), triethyl gallium (TEGa), and water were used as Zn, In, Ga and oxygen precursors, respectively. The vaporized metal precursors have been coinjected in the reactor. The metal composition of InGaZnO has been controlled by varying the TMIn or TEGa flow to the reactor, for a given DEZ flow and exposure time. The morphology of the films changes from polycrystalline, for ZnO and In-doped ZnO, to amorphous for In-rich IZO and InGaZnO. The use of these films as the active channel in TFTs has been demonstrated and the influence of In and Ga cations on the electrical characteristics of the TFTs has been studied.

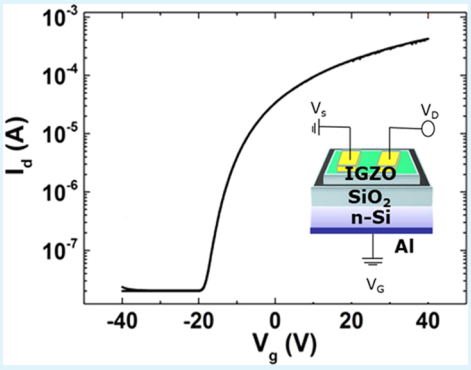


**KEYWORDS:** *atomic layer deposition, atmospheric pressure, thin film transistors, indium gallium zinc oxide, amorphous semiconductors, nucleation*

## INTRODUCTION

Amorphous oxide semiconductors (AOS) are emerging as a novel class of materials for thin-film-transistor (TFT) displays because of their superior electrical properties compared to a-Si:H and better uniformity over large areas than poly-Si based TFTs.[1−4] AOS are based on ternary and quaternary zinc compounds (e.g., InGaZnO, ZnSnO), and their electrical properties can be fine-tuned by varying the composition ratio of metal ions. Amorphous indium gallium zinc oxide (*a*-InGaZnO) is the most widely utilized AOS for the active channel in TFTs due to its reasonably large mobility ($\mu$ > 10 $cm^2/(V\ s)$), low off-currents due to good controllability of the carrier concentration over a wide range ($10^{15}$−$10^{19}$ $cm^{-3}$), and long-term stability.[5,6]

The growth of *a*-IGZO was initially studied using pulsed layer deposition (PLD).[5] PLD allows facile screening of different stoichiometry of the film composition but suffers from poor control of film thickness and composition over a large area. Hence, sputtering is currently most widely used,[1] even though sputtering suffers from a low deposition rate (~0.1 nm/s) and the presence of high-energy species (e.g., ions) can induce defects at the dielectric/semiconductor interface. Solution processing methods have been proposed to decrease the production costs of *a*-InGaZnO, but TFTs with nonoptimal electrical properties have been achieved so far.[7] In this work, we propose the use of spatial atmospheric atomic layer deposition (S-ALD). S-ALD has emerged as a potentially disruptive manufacturing method for the display industry, combining high deposition rates (up to nm/s) with excellent control of film composition and superior uniformity over a large area and even nonflat substrates.[8] Selective S-ALD of metal oxides on patterned surfaces has been recently demonstrated.[9] In this Article, we investigate the nucleation and growth of *a*-InGaZnO by S-ALD and its application as an active channel of TFTs.

Conventionally, the ALD technique is characterized by a time-sequenced introduction of the precursors in the deposition zone, where selective and self-limiting half-reactions occur on the substrate, thus allowing a digital control of the film thickness. S-ALD of metal oxides is performed by sequentially exposing the substrate to an oxygen and a metal precursor which are spatially separated in the ALD injector. Time-consuming purge steps are no longer needed and deposition rates up to a hundred times faster than conventional ALD can be achieved.[10,11] By coinjecting the evaporated metal precursors in the same deposition region, multimetal oxides with uniform distribution of the metal elements along the growth direction have been grown by S-ALD.[12,13]

## EXPERIMENTAL SECTION

A schematic and a description of the S-ALD deposition equipment used in this work can be found in ref 10. Diethyl zinc [$Zn(C_2H_5)_2$, (DEZ)], trimethyl indium [$In(CH_3)_3$, (TMIn)], triethyl gallium

**Received:** November 20, 2014
**Accepted:** January 21, 2015
**Published:** January 21, 2015





DOI: 10.1021/am508071y
*ACS Appl. Mater. Interfaces* 2015, 7, 3671−3675

[$Ga(C_2H_5)_3$, TEGa], and water ($H_2O$) vapor have been selected as zinc, indium, gallium, and oxygen precursors, respectively. DEZ, TMIn, and TEGa are used because of their high vapor pressures and commercial availability. Metal precursors and deionized water were evaporated from bubblers, using argon as carrier gas and transported to the reactor injection head through heated lines, to prevent condensation. The DEZ, TMIn, and TEGa bubblers were kept at room temperature, while the $H_2O$ bubbler is heated to 50 °C. The flows from the DEZ, TMIn, and TEGa bubblers were mixed and injected in the deposition zone through the same inlet, after being diluted by argon. The films have been deposited at a temperature of 200 °C. The exposure time to both the metal precursors and water has been varied in the range from 20 to 120 ms by decreasing the rotation frequency of the substrate from 150 to 25 rotations per minute, respectively.

A Philips X-pert SR5068 powder diffractometer equipped with a Cu K$\alpha$ source was used to determine the crystallographic structure of the films. The film thickness was measured by ex situ spectroscopic ellipsometry measurements, using a J.A. Woollam M2000 rotating compensator ellipsometer in the 300−1000 nm range. The composition of the films was measured in a FEI Quanta 600 FEG SEM system equipped with an energy-dispersive X-ray (EDX) diagnostic, in a Quantera system from ULVAC-PHI (Q2) equipped with X-ray photoelectron spectroscopy (XPS), and by low energy ion scattering spectrometry in an ION-TOF GmbH Qtac100 system (3 keV $He^+$ and 5 keV $Ne^+$ ions are used to quantify the O, Si, C and Zn, In, Ga content, respectively).

Bottom-gate, top-contact InGaZnO TFTs were fabricated on heavily doped *p*-type Si wafers coated by a 300 nm thick thermally grown $SiO_2$, acting as gate dielectric. The source and drain electrodes consisted of Ti (5 nm)/Au (50 nm) layers deposited by electron-beam evaporation. The source-drain electrodes formed a channel measuring approximately 1 mm in width and 50 $\mu$m in length ($W/L$ = 20). The TFTs were electrically characterized in air at room temperature in ambient light.

## RESULTS AND DISCUSSION

Figure 1 shows the film thickness versus number of cycles for various mixtures of metal precursors. No film formation was observed when using TMIn/$H_2O$ (Figure 1a) or TEGa/$H_2O$ (Figure1b), respectively. In the case of DEZ/$H_2O$, the film thickness increases linearly with the number of cycles (Figure 1a). From the slope of this line, a growth per cycle (GPC) of ~0.18 nm/cycle can be calculated which is in agreement with previous results reported in literature for ALD of ZnO.[10] For the deposition conditions used in this paper, ZnO films grow in an ALD mode, where the GPC remains constant with increasing either exposure time or precursors flows, as reported in refs 11−13.

When TMIn and TEGa are coinjected with DEZ, film growth is observed. GPC is typically lower than for the case of DEZ/$H_2O$. When increasing the TMIn partial pressure from 0 to 0.25 mbar at a constant value of DEZ partial pressure of 1.96 mbar, the final thickness is decreased from 250 to 60 nm after 1400 cycles and the GPC does not increase linearly with the number of cycles. The In-content in these films was measured by EDX to increase up to 23% for the highest TMIn/DEZ ratio. When TEGa is added to this mixture (0.25 mbar TMIn, 1.96 mbar DEZ partial pressure), Ga is incorporated into the film. For the highest partial pressure of TEGa of 0.37 mbar, the Ga-content measured by EDX is ca. 30%. These results show that it is possible to grow InGaZnO films by coinjecting the vaporized metal precursors.

Compared to ZnO films, which show a constant film growth, the increase in film thickness with number of cycles reflects a more complex behavior in case of coinjected metal precursors.

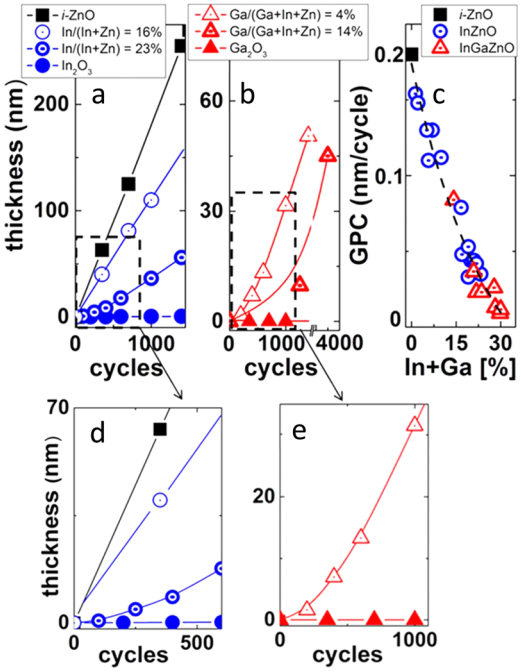


**Figure 1.** Film thickness versus number of ALD cycles for (a) ZnO (■), InZnO (●), (b) InGaZnO (▲), (c) growth per cycle (GPC) of ZnO (■), InZnO (●), and InGaZnO (▲) versus the (In + Ga)/(In + Ga + Zn) ratio, (d) detail of (a), and (e) detail of (b). Film thickness was measured using spectroscopic ellipsometry. The metal composition of the films has been measured by the EDX technique.

A nucleation period of about 200 ALD cycles is observed in In-rich InZnO and in InGaZnO, before the onset of film growth (see Figure 1d,e). As shown in Figure 1c, the GPC of InZnO and InGaZnO decreases with increasing In- and Ga-content. These results suggest that the In- and Ga-atoms on the film surface are not available sites for subsequent film growth.

The nucleation of InZnO has been investigated by the low energy ion scattering (LEIS) technique.[14,15] This technique is used to measure the atomic composition of the outer atomic layer, thus precisely of the atoms which control adsorption and growth. InZnO has been deposited on *p*-type Si substrates coated by thermally grown $SiO_2$. The results are plotted in Figure 2a,b. With an increasing number of ALD cycles from 12 to 150, the surface coverage of $InO_x$ and $ZnO_x$ rises up to the level corresponding to the concentration of the metal elements on the surface of a 40 nm thick InZnO film (i.e., 2000 ALD cycles). The surface coverage of $InO_x$ and $ZnO_x$ after 6 ALD cycles is higher than for the subsequent few cycles, reflecting the density of nucleation sites on the $SiO_2$ substrate, as also reported in ref 16. During the first 150 ALD cycles, part of the surface is formed by $SiO_2$ thus indicating that film closure is not achieved yet. In this phase, the film surface is rich in In-atoms, while an In/In + Zn ratio of about 30% is measured on the surface of a closed InZnO film (see Figure 2a).

The bulk composition of the InZnO and InGaZnO as determined by XPS depth profiling is shown in Figure 2c,d. For the settings used in the XPS analysis, the atomic distribution of the different elements (In, Zn, Ga, O, C) can be measured along the growth direction with a resolution of ~7 nm.[12] A nearly constant concentration-depth profile for In, Ga, and Zn elements is measured in the films, within the resolution limit of the XPS analysis. In both films, the carbon concentration is


DOI: 10.1021/am508071y
ACS Appl. Mater. Interfaces 2015, 7, 3671−3675

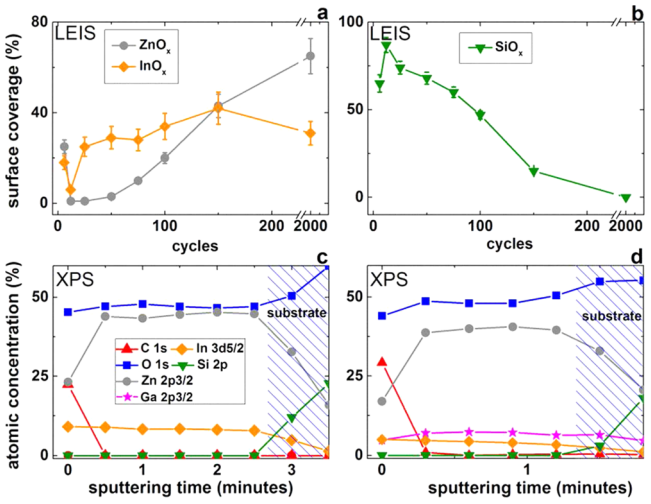


**Figure 2.** Surface coverage of (a) $InO_x$, $ZnO_x$ and (b) $SiO_x$ for InZnO grown on $SiO_2$ substrate versus number of ALD cycles measured by the LEIS technique. Bulk composition of (c) 20 nm thick IZO and (d) 15 nm thick IGZO measured by XPS depth profiling.

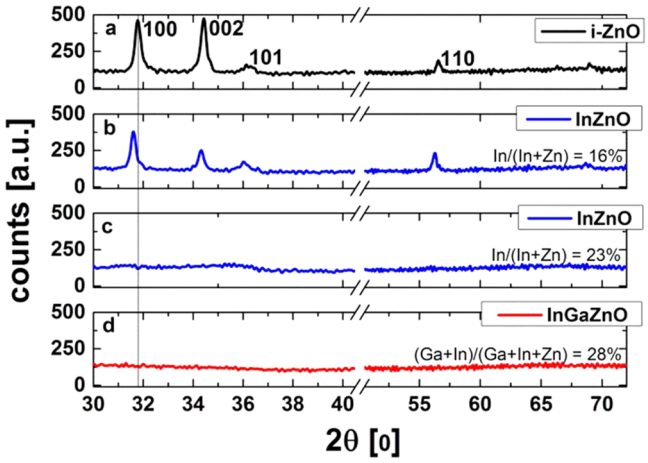


**Figure 3.** XRD spectra of as deposited (a) ZnO, (b and c) InZnO, and (d) InGaZnO. The metal composition of the films has been measured by EDX.

below the detection limit after sputter removal of the top layers that were exposed to the atmosphere prior to analysis.

ALD of ZnO, $In_2O_3$, and $Ga_2O_3$ has been extensively investigated in literature. DEZ and water are commonly used precursors for ALD and S-ALD of ZnO.[11] Ritala et al. did not obtain the growth of $In_2O_3$ using TMIn and $H_2O$.[17] Ott et al. proposed that the ALD growth of $In_2O_3$ is hindered by the low reactivity between TMIn and surface hydroxyl groups.[18] Chalker et al.[20] did not detect any growth of $Ga_2O_3$ by using TEGa and $H_2O$, but the growth of ZnGaO was achieved when coinjecting DEZ and TEGa.[19] Similarly, we observe the growth of InZnO and InGaZnO when coinjecting DEZ, TMIn, and TEGa in the deposition zone, although the use of TMIn/$H_2O$ and TEGa/$H_2O$ does not result in any deposition.

Spontaneous homogeneous reactions between gas phase reactants (e.g., DEZ with TMIn or TEGa) are energetically not (or less) probable at the moderate temperatures used in our experiments. It is more likely that, once a DEZ molecule has adsorbed and fragmented at the substrate surface, an activated transition state forms which is reactive enough to cause polarity-induced dissociation of the metal−ligand bond of a TMIn or TEGa molecule impinging on this reactive surface entity.[20]

The absence of carbon contamination from the bulk of InZnO and InGaZnO indicates that methyl groups bonded to In- and Ga-atoms are effectively removed from the surface of the film via a ligand exchange reaction with water molecules. A high Langmuir exposure to water (~3 Torr·s) has been used to fully react the surface methyl groups.[21,22] The possibility of growing $In_2O_3$ or $Ga_2O_3$ by further increasing the Langmuir exposure to water is currently under investigation. The low reactivity of either Ga-$CH_3$ groups with water or surface hydroxyl groups bonded to In- and Ga-atoms with the metal precursors, the formation of bridge M−O−M bonds (M = In, Ga), or steric hindrance induced by In$(CH_3)_x$ and Ga$(CH_3)_x$ fragments can result in a long nucleation period and in a decrease of the GPC of InGaZnO, as we measure with increasing In- or Ga-content (see Figure 1).[18,23]

XRD spectra of ZnO, InZnO, and InGaZnO are shown in Figure 3. ZnO has a poly crystalline structure with (002) and (100) main orientations, as commonly reported for films grown by S-ALD.[11] The incorporation of In-atoms in the ZnO lattice induces a decrease in the intensity of the crystalline peaks and a shift of the (100) peak positions toward lower angles. This indicates the formation of tensile stress in the film, possibly because of the creation of crystallographic defects (e.g., zinc vacancies or interstitials) in the ZnO lattice. A further increase in In-content (i.e., In/(Zn + In) = 23%) results in films with an amorphous structure.[24]

The deposition of amorphous InZnO has been reported by sputtering and conventional ALD.[21,22,24] A transition from polycrystalline to amorphous morphology is typically observed in sputtered InZnO for an In-content of ~40%.[25] Similar results are reported for ALD InZnO grown from supercycles of ZnO and $In_2O_3$ binary oxides.[21,22] For the deposition conditions reported in this paper, In-atoms are incorporated in ZnO, but they are not available as active surface sites for consecutive film growth. In-atoms can disrupt the local growth of ZnO crystals, inducing a transition to an amorphous phase at a much lower In-content than reported for sputtering or conventional ALD. InGaZnO films with (In + Ga)/(In + Ga + Zn) = 28% have an amorphous structure, as shown in Figure 3d.

S-ALD *a*-IGZO has been tested as active channel material in TFTs. Fifteen nm thick *a*-IGZO was deposited on highly doped *p*-type Si substrate coated by 300 nm thick thermally grown $SiO_2$ dielectric. The samples were then annealed in ambient atmosphere at 450 °C for 1 h. XRD spectra indicate that S-ALD *a*-IGZO maintains an amorphous structure after annealing (not shown). Postdeposition annealing up to 500 °C in air is known to enhance the electron mobility in *a*-IGZO by removing trap states near the conduction band minimum, which hinders the electron transport.[26−28] The devices were then annealed at 100 °C in an ambient atmosphere for 1 h to optimize the electrical contacts of the IGZO films with the source and drain electrodes.

Figure 4a shows the transfer characteristics ($I_{DS}$ − $V_{DS}$ sweep) of a TFT with Ga/(In + Ga + Zn) = 8% and In/(In + Ga + Zn) = 20%. The current $I_{DS}$ markedly increases at a positive gate bias ($V_{GD}$), indicating that the channel is *n*-type. The $I_{DS}$ − $V_{DS}$ characteristics exhibit a clear pinch-off and current saturation. The estimated value of the field effect mobility ($\mu_{FE}$) is about 3.5 $cm^2/(V\ s)$, which is a factor of 3 lower than the mobility values typically reported for sputtered


DOI: 10.1021/am508071y
ACS Appl. Mater. Interfaces 2015, 7, 3671−3675

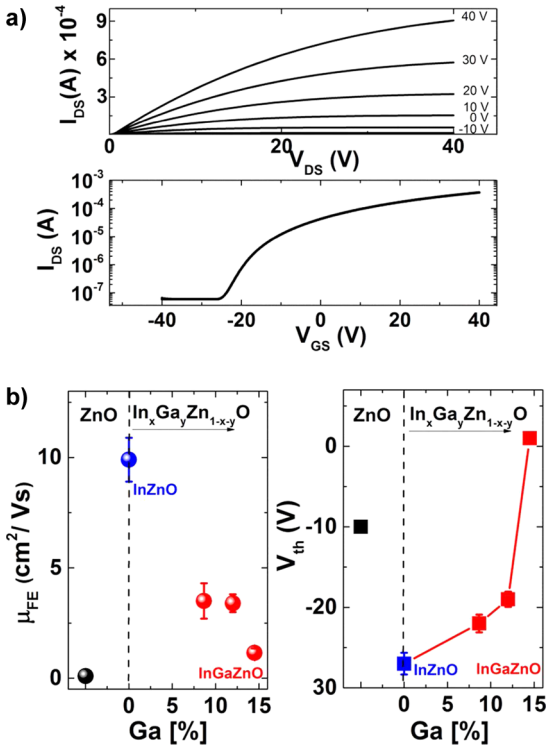


**Figure 4.** (a) $I_{DS}$ versus $V_{GS}$, $I_{DS}$ versus $V_{GS}$ of TFTs with a spatial ALD *a*-InGaZnO active channel for Ga/(Ga + In + Zn) = 8% and In/(Ga + In + Zn) = 20%. (b) $V_{th}$ and $\mu_{FE}$ of TFTs with ZnO, *a*-IZO (In/(In + Zn) = 27%), and an *a*-InGaZnO active channel with In/(Ga + In + Zn) = 20%, 24%, 15%, and Ga/(Ga + In + Zn) = 8%, 12%, 14%, respectively. All films have been deposited with a constant exposure time to vaporized metal and oxygen precursors of 120 ms. The metal composition of the films has been measured by EDX.

*a*-IGZO transistors. The negative onset voltage (−25 V) implies a relatively high density of free carriers (>$10^{17}$ $cm^{-3}$).[29] The transfer characteristics show little to no hysteresis suggesting that the device is very stable. This has been confirmed via bias stress measurements in air where the nonpassivated InGaZnO TFTs displayed a remarkable low threshold voltage shift of <0.2 V in both positive and negative directions under applied gate fields of ±1 MV/cm. Bias induced threshold shifts are commonly attributed to back channel effects in these devices, such as high density of defects at the dielectric/semiconductor interface. The good bias stress stability therefore is in line with our original assumption that S-ALD is a "soft" deposition technique.[30]

Next, we have investigated the influence of gallium and indium cations on the electrical characteristics (i.e., $\mu_{FE}$, $V_{th}$) of the TFTs. As shown in Figure 4b, ZnO TFTs have a negative threshold voltage ($V_{th}$ = −10 V) and a low field effect mobility ($\mu_{FE}$ = 0.1 $cm^2$/(V s)).[31−33] The incorporation of In-atoms in the ZnO lattice (In/(In + Zn) = 27%) results in a sharp increase of field effect mobility (10 $cm^2$/(V s)) and in a lower negative threshold voltage (−27 V) than for bare ZnO TFTs (Figure 4b). According to the literature, a higher field effect mobility is generally measured when increasing In-content in the *a*-InZnO active channel. This is observed for *a*-InZnO grown by several techniques, as sputtering, solution processing, or pulsed laser deposition.[34−36] Density functional theoretical studies report that In 5s electrons are the majority carriers in *a*-InZnO and *a*-InGaZnO.[36,37] Localized Zn-vacancies can act as hopping centers between In 5s orbitals, thus promoting the electron transport.[37] The overlapping of neighboring s orbitals originating in the $In^{3+}$-cations, whose s orbitals are larger than that of $Zn^{2+}$, enhances the electron mobility.[1] In-substitution of the Zn-sites provides excess electron carriers in addition to those generated by intrinsic defects, which makes $V_{th}$ more negative than that for bare ZnO TFTs.

The threshold voltage rises from −27 V up to 1 V with increasing the Ga-content from 0% to 15%, respectively, as shown in Figure 4b. Ga-ions form stronger chemical bonds with oxygen than with Zn- and In-ions because of their high ionic potential, due to their +3 valence and small ionic radius.[36] Therefore, Ga-ions hinder the formation of oxygen vacancies, suppressing the generation of free carriers so that the value of the threshold voltage of TFTs increases. In line with Iwasaki et al., we measure a decrease in field effect mobility with higher Ga-content (see Figure 4b).[35] The random distribution of $Ga^{3+}$-ions in the *a*-InGaZnO lattice modulates the electronic structure around the conduction band edge, creating a statistical distribution of potential barriers, which hinder the electron transport.[38]

## CONCLUSIONS

In summary, we investigated the growth of *a*-InGaZnO by atmospheric S-ALD and the effect of the chemical composition of In- and Ga-cations on the electrical characteristics of TFTs. Although the nonideal surface kinetics between vaporized metal precursors and water hinders the growth of $In_2O_3$ and $Ga_2O_3$, *a*-InGaZnO has been deposited by coinjecting DEZ, TMIn, and TEGa. The influence of In- and Ga-cations on the electrical characteristics of *a*-InGaZnO TFTs is similar to that reported in the literature for other deposition techniques, such as sputtering, solutions processing, and pulsed laser deposition. These results show the viability of atmospheric S-ALD as a new manufacturing technique for low-cost and large-area electronics based on amorphous oxide semiconductors.

## AUTHOR INFORMATION

### Corresponding Author

*E-mail: andrea.illiberi@tno.nl.

### Notes

The authors declare no competing financial interest.

## REFERENCES

(1) Ginley, D., Hosono, H., Paine, C. D., Eds. *Handbook of Transparent Conductors*; Springer Series in Materials Science: New York, 2011.

(2) Kamiya, T.; Nomura, K.; Hosono, H. Origins of High Mobility and Low Operation Voltage of Amorphous Oxide TFTs: Electronic Structure, Electron Transport, Defects and Doping. *J. Disp. Technol.* **2009**, *5*, 273−288.

(3) Kamiya, T.; Hosono, H. Material Characteristics and Applications of Transparent Amorphous Oxide Semiconductors. *NPG Asia Mater.* **2010**, *2*, 15−22.

(4) Fortunato, E. M. C.; Pereira, L. M. N.; Barquinha, P. M. C.; Botelho do Rego, A. M.; Goncalves, G.; Vila, A.; Morante, J. R.; Martins, R. F. P. High Mobility Indium Free Amorphous Oxide Thin Film Transistors. *Appl. Phys. Lett.* **2008**, *92*, 222103.

(5) Nomura, K.; Ohta, H.; Takagi, A.; Kamiya, T.; Hirano, M.; Hosono, H. Room-Temperature Fabrication of Transparent Flexible Thin-Film Transistors Using Amorphous Oxide Semiconductors. *Nature* **2004**, *432*, 488−492.



DOI: 10.1021/am508071y
*ACS Appl. Mater. Interfaces* 2015, 7, 3671−3675

(6) Yaglioglu, B.; Yeom, H. Y.; Beresford, H. Y.; Paine, D. C. High-Mobility Amorphous $In_2O_3$-10 wt % ZnO Thin Film Transistors. *Appl. Phys. Lett.* **2006**, *89*, 062103.
(7) Fortunato, E.; Barquinha, P.; Martins, R. Oxide Semiconductor Thin-Film Transistors: A Review of Recent Advances. *Adv. Mater.* **2012**, *24*, 2945−2986.
(8) Poodt, P.; Cameron, D. C.; Dickey, E.; George, S. M.; Kuznetsov, V.; Parsons, G. N.; Roozeboom, F.; Sundaram, G.; Vermeer, A. Spatial Atomic Layer Deposition: A Route Towards Further Industrialization of Atomic Layer Deposition. *J. Vac. Sci. Technol., A* **2012**, *30*, 010802.
(9) Ellinger, C. R.; Nelson, S. F. Selective Area Spatial Atomic Layer Deposition of ZnO, $Al_2O_3$, and Aluminum-Doped ZnO Using Poly(vinyl pyrrolidone). *Chem. Mater.* **2014**, *26*, 1514−1522.
(10) Poodt, P.; Lankhorst, A.; Roozeboom, F.; Spee, K.; Maas, D.; Vermeer, A. High-Speed Spatial Atomic-Layer Deposition of Aluminum Oxide Layers for Solar Cell Passivation. *Adv. Mater.* **2010**, *22*, 3564−3567.
(11) Illiberi, A.; Roozeboom, F.; Poodt, P. Spatial Atomic Layer Deposition of Zinc Oxide Thin Films. *ACS Appl. Mater. Interfaces* **2012**, *4*, 268−272.
(12) Illiberi, A.; Scherpenborg, R.; Wu, Y.; Roozeboom, F.; Poodt, P. Spatial Atmospheric Atomic Layer Deposition of $Al_xZn_{1-x}O$. *ACS Appl. Mater. Interfaces* **2014**, *5*, 13124−13128.
(13) Illiberi, A.; Poodt, P.; Bolt, P. J.; Roozeboom, F. Recent Advances in Atmospheric Vapor-Phase Deposition of Transparent and Conductive Zinc Oxide. *Chem. Vap. Deposition* **2014**, *20*, 234−242.
(14) Brongersma, H. H.; Draxler, M.; de Ridder, M.; Bauer, P. Surface Composition Analysis by Low-Energy Ion Scattering. *Surf. Sci. Rep.* **2007**, *62*, 63−109.
(15) Brongersma, H. H. In *Characterization of Materials*; J. Wiley & Sons: Hoboken, NJ, 2012; pp 2024−2044.
(16) Libera, J. A.; Hryn, J. N.; Elam, J. W. Indium Oxide Atomic Layer Deposition Facilitated by the Synergy Between Oxygen and Water. *Chem. Mater.* **2011**, *23*, 2150−2158.
(17) Ritala, M.; Asikainen, T.; Leskelä, M.; Skarp, J. Ale Growth of Transparent Conductors. *Mater. Res. Soc. Symp. Proc.* **1996**, *426*, 513−518.
(18) Ott, A. W.; Johnson, J. M.; Klaus, J. W.; George, S. M. Surface Chemistry of $In_2O_3$ Deposition Using $In(CH_3)_{(3)}$ and $H_2O$ in a Binary Reaction Sequence. *Appl. Surf. Sci.* **1997**, *112*, 205−215.
(19) Saito, K.; Hiratsuka, Y.; Omata, A.; Makino, H.; Kishimoto, S.; Yamamoto, T.; Horiuchi, N.; Hirayama, H. Atomic Layer Deposition and Characterization of Ga-Doped ZnO Thin Films. *Superlattices Microstruct.* **2007**, *42*, 172−175.
(20) Chalker, P. R.; Marshall, P. A.; Romani, S.; Roberts, J. W.; Irvine, S. J. C.; Lamb, D. A.; Clayton, A. J.; Williams, P. A. Atomic Layer Deposition of Ga-doped ZnO Transparent Conducting Oxide Substrates for CdTe-Based Photovoltaics. *J. Vac. Sci. Technol., A* **2013**, *31*, 01A120.
(21) Lee, D. J.; Kwon, J. Y.; Lee, J. I.; Kim, K. B. Self-Limiting Film Growth of Transparent Conducting $In_2O_3$ by Atomic Layer Deposition Using Trimethylindium and Water Vapor. *J. Phys. Chem. C* **2011**, *115*, 15384−15389.
(22) Lee, D. J.; Kwon, J. Y.; Kim, J.; Kim, K. J.; Cho, Y. H.; Cho, S. Y.; Kim, S. H.; Xu, J.; Kim, K. B. Ultrasmooth, High Electron Mobility Amorphous In-Zn-O Films Grown by Atomic Layer Deposition. *J. Phys. Chem. C* **2014**, *118*, 408−415.
(23) Comstock, D. J.; Elam, J. W. Atomic Layer Deposition of $Ga_2O_3$ Films Using Trimethylgallium and Ozone. *Chem. Mater.* **2012**, *24*, 4011−4018.
(24) Illiberi, A.; Scherpenborg, R.; Roozeboom, F.; Poodt, P. Atmospheric Spatial Atomic Layer Deposition of In-Doped ZnO. *ECS J. Solid State Sci. Technol.* **2014**, *3*, P111−P114 [24].
(25) Taylor, M. P.; Readey, D. W.; van Hest, M. F. A. M.; Teplin, C. W.; Alleman, J. L.; Dabney, M. S.; Gedvilas, L. M.; Keyes, B. M.; To, B.; Perkins, J. D.; Ginley, D. S. The Remarkable Thermal Stability of Amorphous In-Zn-O Transparent Conductors. *Adv. Funct. Mater.* **2008**, *18*, 3169−3178.
(26) Nomura, K.; Kamiya, T.; Ohta, H.; Shimizu, K.; Hirano, M.; Hosono, H. Relationship Between Non-localized Tail States and Carrier Transport in Amorphous Oxide Semiconductor, In−Ga−Zn−O. *Phys. Status Solidi A* **2008**, *205*, 1910−1914.
(27) Nomura, K.; Kamiya, T.; Ohta, H.; Ueda, K.; Hirano, M.; Hosono, H. Carrier Transport in Transparent Oxide Semiconductor with Intrinsic Structural Randomness Probed Using Single-Crystalline $InGaO_3(ZnO)_{(5)}$ Films. *Appl. Phys. Lett.* **2004**, *85*, 1993−1995.
(28) Hosono, H.; Nomura, K.; Ogo, Y.; Uruga, T.; Kamiya, T. Factors Controlling Electron Transport Properties in Transparent Amorphous Oxide Semiconductors. *J. Non-Cryst. Solids* **2008**, *354*, 2796−2800.
(29) Kamiya, T.; Nomura, K.; Hirano, M.; Hosono, H. Electronic Structure of Oxygen Deficient Amorphous Oxide Semiconductor a-$InGaZnO_{4-x}$: Optical Analyses and First-Principle Calculations. *Phys. Status Solidi C* **2008**, *5*, 3098−3100.
(30) Trinh, T. T.; Nguyen, V. D.; Ryu, K.; Jang, K.; Lee, W.; Baek, S.; Raja, J.; Yi, J. Improvement in the Performance of an InGaZnO Thin-Film Transistor by Controlling Interface Trap Densities Between the Insulator and Active Layer. *Semicond. Sci. Technol.* **2011**, *26*, 085012.
(31) Levy, D. H.; Nelson, S. F. Thin-Film Electronics by Atomic Layer Deposition. *J. Vac. Sci. Technol., A* **2012**, *30*, 018501.
(32) Levy, D. H.; Freeman, D.; Nelson, S. F.; Cowdery-Corvan, P. J.; Irving, L. M. Stable ZnO Thin Film Transistors by Fast Open Air Atomic Layer Deposition. *Appl. Phys. Lett.* **2008**, *92*, 192101.
(33) Levy, D. H.; Nelson, S. F.; Freeman, D. Oxide Electronics by Spatial Atomic Layer Deposition. *J. Display Technol.* **2009**, *5*, 484−494.
(34) Kim, Y. H.; Han, M. K.; Han, J. I.; Park, S. K. Effect of Metallic Composition on Electrical Properties of Solution-Processed Indium-Gallium-Zinc-Oxide Thin-Film Transistors. *IEEE Trans. Electron Devices* **2010**, *57*, 1009−1014.
(35) Iwasaki, T.; Itagaki, N.; Den, T.; Kumomi, H.; Nomura, K.; Kamiya, T.; Hosono, H. Combinatorial Approach to Thin-Film Transistors Using Multicomponent Semiconductor Channels: An Application to Amorphous Oxide Semiconductors in In−Ga−Zn−O System. *Appl. Phys. Lett.* **2007**, *90*, 242114.
(36) Nomura, K.; Kamiya, T.; Ohta, H.; Uruga, T.; Hirano, M.; Hosono, H. Local Coordination Structure and Electronic Structure of the Large Electron Mobility Amorphous Oxide Semiconductor In-Ga-Zn-O: Experiment and ab Initio Calculations. *Phys. Rev. B* **2007**, *75*, 035212.
(37) Orita, M.; Tanji, H.; Mizuno, M.; Adachi, H.; Tanaka, I. Mechanism of Electrical Conductivity of Transparent $InGaZnO_4$. *Phys. Rev. B* **2006**, *61*, 1811.
(38) Cho, D. Y.; Song, J.; Na, K. D.; Hwang, C. S.; Jeong, J. H.; Jeong, J. K.; Mo, Y. G. Local Structure and Conduction Mechanism in Amorphous In−Ga−Zn−O Films. *Appl. Phys. Lett.* **2009**, *94*, 112112.


DOI: 10.1021/am508071y
*ACS Appl. Mater. Interfaces* 2015, 7, 3671−3675